

## 3D Bio-Plotted Composite Scaffold Made of Collagen Treated Hydroxyapatite-Tricalciumphosphate for Rabbit Tibia Bone Regeneration

Pranav S. Sapkal<sup>1\*</sup>, Abhaykumar M. Kuthe<sup>1</sup>, Divya Ganapathy<sup>2</sup>, Shantanu C. Mathankar<sup>3</sup> and Sudhanshu Kuthe<sup>4</sup>

**Abstract:** Biphasic calcium phosphate scaffolds with 20/80 HA/TCP ratio were fabricated using the 3D-Bioplotting system to heal critical size defects in rabbit tibia bone. Four different architectures were printed in a layer by layer fashion with lay down patterns viz. (a) 0°-90°, (b) 0°-45°-90°-135°, (c) 0°-108°-216° and (d) 0°-60°-120°. After high-temperature sintering scaffolds were coated with collagen and were further characterized by (FTIR) Fourier Transform Infrared Spectroscopy, (SEM) Scanning Electron Microscopy, (XRD) X-Ray diffraction, Porosity analysis and Mechanical testing. Scaffold samples were tested for its ability to induce cytotoxicity in Balb/c 3T3 cells at in vitro condition using elution method. Skin sensitization potential of scaffolds was evaluated in male guinea pigs using guinea pig maximization test (GPMT). Further, scaffolds were implanted in eight rabbit tibia bones and biocompatibility and histological evaluations were carried out after 4 and 8 weeks implantation periods. In-vitro results include bonding, surface morphology, phases, porosity, mechanical strength and Cytotoxicity. In-vivo results include sensitization, capsule formation, inflammation, presence of polymorphonuclear cells, giant cells, plasma cells, X-Rays and degradation of the material. It was concluded that HA/TCP/Collagen scaffold with 0°-45°-90°-135° architecture exhibits the most excellent properties in healing critical size bone defects in rabbits.

**Keywords:** BCP (Biphasic Calcium Phosphate), MSC (Mesenchymal Stem Cell), in vitro, in-vivo.

### 1 Introduction

Application of material science, particularly use of biomaterials in the field of health care and reconstructive surgery is one of the most exciting and challenging areas in the present world [Ratner, Hoffman, Schoen et al. (2004)]. Biomaterials are synthetic materials

---

<sup>1</sup>Department of Mechanical Engineering, Visvesvaraya National Institute of Technology, Nagpur, India.

<sup>2</sup>CEO and Founder at Regulatory1, Bengaluru, India.

<sup>3</sup>Department of Biochemical Engineering and Biotechnology, Indian Institute of Technology, Delhi, India.

<sup>4</sup>Department of Metallurgical & Materials Engineering, Visvesvaraya National Institute of Technology, Nagpur, India.

\*Corresponding Author: Pranav S. Sapkal- pranav\_sapkal@rediffmail.com

known for their ability to withstanding a biological environment without inducing any adverse effects on the surrounding tissues [Valiathan and Krishnan(1999)]. Among different biomaterials, metals and alloys are used in dentistry, orthopedics and load bearing applications. Ceramics because of its high bioactive property and chemically inert nature are also used for osseous tissue replacement. Polymeric materials use is restricted to soft tissues replacements like blood vessels, heart valve, intraocular lenses and cranial areas [Hench and Wilson; Park and Bronzino (2003); Piconi and Maccauro (1999); Hench (1998)]. Out of the above applications for biomaterials, bone tissue replacement is of significant importance as it protects vital organs and holds body structure. Also, it is established that worldwide millions of people do suffer from bone related issues which include sudden fractures and degeneration. It is apprehended that by the year 2020 twice the number of people, above 50 years of age will be facing this problem as compared to today [Sapkal, Kuthe and Kashyap et al. (2016)]. The treatments available to these problems are autografts, allograft and xenograft. Autologous bone graft is a viable option but substituting graft from one site to other obstructs the functioning at the original site. The allogenic and xenogenic source might face rejection and disease transmission issues [Yang, Leong, Duet al. (2001)]. The metallic implant which is currently being used for total hip and knee joint replacements also encounter problems like re-surgery, chronic irritation, dislocation from the site and implant loosening.

In the past, calcium phosphate ceramics has been used as bone filling material and also for various orthopedic joint replacements. First successful application of calcium phosphate for bone repair in humans was reported in 1920 [Albee (1920)]. However, after 50 years in 1980's and 90's, extensive studies were carried out on apatites (especially calcium hydroxyapatite, HA) and calcium phosphates (particularly  $\beta$ -TCP) for their potential use as bone substitute material [Aoki (1994);DeGroot (1983);Jarcho (1981)]. HA, which has a similar mineral composition as that of bone and teeth, is extensively studied for applications requiring bioactive property. However, its slow degradation and poor mechanical properties limit its use in load-bearing sites as bulk monolithic materials [Sun and Lal (2002);Ye, Yang, et al. (2012);Oliveira Lomelino, Castro-Silva, Linhares, et al. (2012);Sharaf, Faris, Abukawa, et al. (2011)]. BCP bioceramic which is a mixture of more stable HA phase and more soluble TCP phase provides optimal balance through the gradual dissolution through the release of calcium and phosphate ions in the biological environment and simultaneous bone formation [Daculsi, LeGeros, Nery et al. (1989)].

Presently, commercial BCPs are available in the market with varying HA/TCP ratios and are sold as bone substitute material for dental and orthopedic applications. Interconnecting macroporosity and appropriate microporosity are two significant physical properties that are required for optimum biological performance in bioceramic dissolution, bioceramic-cell interaction, bioceramic-tissue interface and new bone formation [LeGeros (2002); Goyenvalle, Aguado and Legeros et al. (2007)]. Minimum microporosity of 20% is necessary for optimal ability of BCP, as low microporosity can lead to lesser bioactivity and lesser dissolution rate. Also, pore size for a bioceramic material should be similar to that of bone. Micropores of diameter less than 10  $\mu\text{m}$  on the surface are required for body fluid circulation whereas macropores of diameter more than 100  $\mu\text{m}$  are required for bone cell colonization. Conversely, percent macroporosity and pore size will affect the mechanical

properties of the BCP ceramic [LeGeros (2002)]. At the initial stage ceramic properties like composition, porosity, pore size and architecture are more important for bone induction than mechanical stability [Daculsi, LeGeros, Grimandiet al. (2008)]. The increase in micro and macro porosity in BCP ceramics helps in the formation of microcrystals with Ca/P ratios comparable to that of bone apatite crystals. The richness of these crystals is directly related to initial  $\beta$ -TCP/HA ratio in BCP: greater the ratio higher the formation of microcrystal [Daculsi and Dard (1994)]. Different studies have been performed to evaluate the effect of varying ratios of HA/TCP in BCP on tissue ingrowth and bioceramic resorption. Daculsi et al. in his study used HA/TCP ratios of 20/80 and 80/20 for filling maxillofacial defects in dog mandibular with only micropore content and critical size defect (6mm diameter cylindrical samples) in dog femoral epiphyses with macro and microporosity. After four, six and twelve weeks of implantation, no significant difference in bone ingrowth and bioceramic resorption was observed in both the samples at both the sites. Several studies have been published on large size defects in load-bearing bones. Regenerating large size defects in rabbit bones is a challenge, as osteosynthesis should support physiological loading. It has been published that 2 cm defect in rabbit femur is considered as critical size defect for 16 weeks of time [Crigel and Balligand (2002); Hollinger and Kleinschmidt (1990)]. Livingston et al. (2003) in his study used fast resorbable BCP bio-ceramic with 20/80 HA/TCP ratio to heal critical size rabbit defect. Porcine collagen membrane was used to cover the BCP granules as the periosteum was removed. Results showed successful bone growth in composite (BCP+collagen membrane) for rabbit femur [Livingston, Gordon, Archambault, et al. (2003)]. Arinze et al. (2003) did a relative study to find out the optimum HA/TCP ratio in the combination of MSCs that would induce fast and uniform bone formation in-vivo. Results revealed that BCP with lower HA/TCP ratio (20/80) loaded with hMSCs promoted maximum amount of new bone formation inside the porous structure of BCP scaffold. Scaffolds with 100% HA, 100% TCP and higher HA/TCP ratio showed less amount of bone formation after 6 weeks of implantation. Also in the in-vitro study, it was established that hMSCs expressed osteocalcin, a specific bone marker when grown on 20/80 HA/TCP in four week time. The rapid amount of bone formation in-vivo and osteocalcin expression on hMSCs loaded 20/80 HA/TCP ceramic in-vitro may occur due to the fast dissolution rate and the surface chemistry as compared to other BCPs [Livingston, Peter, Archambault, et al. (2003)].

Conventional techniques to make BCP scaffolds include salt leaching, sponge replica, gas foaming, emulsion freeze drying solvent casting etc [Zein, Hutmacher, Tan, et al. (2002)]. The problems associated with the above techniques is that they do not guarantee continuous interconnected porous structure which hampers the osseointegration property of scaffold [Chen, Li and Lu et al. (2005)]. Now with the advent of imaging techniques like computed tomography (CT), Magnetic resonance imaging (MRI), CAD-CAM and rapid manufacturing customized design for scaffold are possible. 3D printing, (SLA) Stereolithography, Selective laser sintering (SLS), Fused deposition modeling (FDM) and 3D-Bioplotting are some of the major technologies that represent rapid manufacturing [Sarkar and Lee. (2015)]. The above techniques ensure interconnected macroporous architecture with predictable mechanical properties. The main aim of the paper is to evaluate the effect of scaffold architecture on the mechanical strength and porosity values of the scaffolds in

order to use it in load bearing sites. BCP scaffolds with 20/80, HA/TCP ratio have been fabricated with four different architectures using the 3D-Bioplotter system: (a) 0°-90°, (b) 0°-45°- 90°-135°, (c) 0°-108°-216° and (d) 0°-60°-120°. After high temperature sintering the samples were treated with collagen and were then characterized according to (FTIR) Fourier Transform Infrared Spectroscopy, (SEM) Scanning Electron Microscopy, (XRD) X-Ray diffraction, porosity analysis and mechanical strength. Finally, the scaffold architecture with maximum mechanical stability and optimum porosity is further tested for its in-vitro (cytotoxicity) and in-vivo (Skin sensitization study on guinea pigs and biocompatibility and histological evaluation of rabbit tibia bone implant with HA/ TCP/ Collagen scaffolds) capabilities.

## 2 Materials & methods

### 2.1 3D-Bioplotting of HA/TCP/collagen scaffolds

$\beta$ -tri-Calcium phosphate (25  $\mu\text{m}$  particle size), Hydroxyapatite nanopowder, (<200 nm particle size) and Collagen from rat tail, Bornstein and Traub Type 1 powder were acquired from Sigma-Aldrich, USA. Polyvinyl alcohol (PVA) was purchased from Fisher Scientific, India. First, the  $\beta$ -TCP powder was sieved through a mesh size of 500 to get uniform particle size of 25  $\mu\text{m}$ . Afterward, nanosize (<200 nm) HA powder was added to TCP at a concentration of 20% by weight. Binder solution was prepared by mixing 3 grams of polyvinyl alcohol (PVA) in 37 grams of water. The solution was stirred for 30 min to get the binder solution which was subsequently sieved to remove suspended particles. Finally, 10 grams of HA/TCP powder was further added to 7 grams of binder solution to get a uniform viscous ceramic paste. The solid freeform process was carried out using 3D-Bioplotter, Developer Series, Envision TEC, Germany Fig.1. The system consists of: (a) paste dispensing unit having syringe and nozzle; (b) air pressure system to control the flow of the ceramic paste; and (c) control unit which is connected to a computer having software (VisualMachines) to regulate the fiber deposition path. The paste was filled in a 30ml PE (Polyethylene) syringe and was placed inside the low-temperature head, which is fixed on the vertical axis of the machine. Air pressure was applied to the plunger, to push the paste outside the nozzle. Rectangular models of size 10mm x 10mm x 3mm were loaded on the (BioplotterRP) software of the machine. Scaffolds were printed in a layer by layer fashion with four different architectures having lay down pattern as (a) 0°-45°-90°-135°, (b) 0°-108°-216°, (c) 0°-90° and (d) 0°-60°-120° Fig.2. Scaffolds were printed using PE plastic nozzle (Nordson, USA) having length 32mm and an inner diameter of 400  $\mu\text{m}$ . For all architecture types, the distance between strands was set to 1mm in order to generate pore size of around 500 to 600  $\mu\text{m}$ . The temperature of the printing head was set to 30°C and the printing was done at a speed of 15mm/s with a pressure of 3.6 bars. The fabricated scaffolds were first allowed to dry at room temperature for 24 hours after which they were kept in the oven for another 24 hours to vaporize the water present in the samples. Afterward, the samples were subjected to the following sintering process in a silicon carbide furnace.

RT  $\rightarrow$  600°C in 480 min  $\rightarrow$  600°C Temp Hold for 120 min  $\rightarrow$  1250°C in 450 min  $\rightarrow$  1250°C Temp Hold for 120 min  $\rightarrow$  furnace cooling RT.

Scaffolds were subsequently coated with collagen. For which the samples were placed inside the collagen solution for 2 hours to infiltrate surface of the strands with collagen. The collagen solution was prepared by adding 5mg of collagen powder in 5ml of 0.1M acetic acid solution. The solution was stirred for 3 hours until dissolved. After collagen coating, the samples were air dried for 3 hours and later washed with PBS (Phosphate Buffer Solution) for four times [Haberstroh, Ritter and Kuschnierzetet al. (2010)].

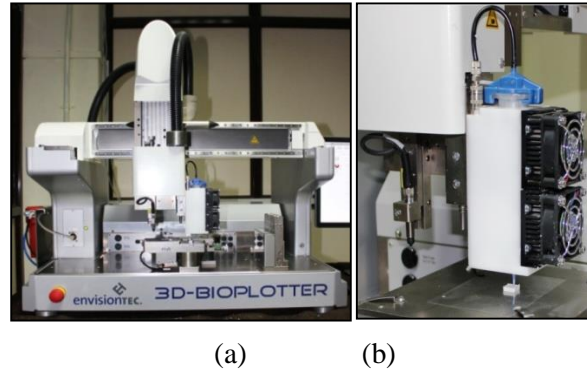


**Figure 1:** 3D-Bioplotting of HA/TCP ceramic: (a) Front view of 3D-Boplotter. (b) Isometric view of scaffold printing.

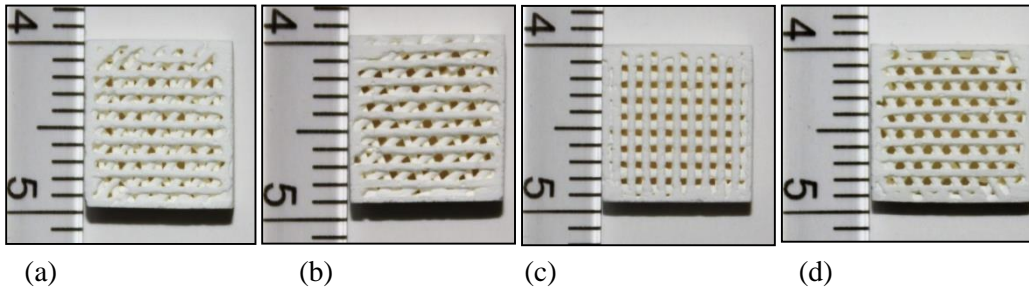


**Figure 2:** Sintered HA/TCP scaffolds with different lay down pattern (a) 0°-45°-90°-135° (b) 0°-108°-216° (c) 0°-90° (d) 0°-60°-120°.

## 2.2 Porosity analysis and mechanical testing of HA/ $\beta$ -TCP scaffolds

The porosity of all four sintered scaffolds with different strand orientations was calculated by using liquid displacement method. Ethanol was used as the displacing liquid because of its high pore penetration capability, also after getting absorbed it does not induce bulging or contraction in the sample. Scaffold sample was immersed in a 15ml Eppendorf tube containing known volume of ethanol ( $V_1$ ). The tube was sealed and the sample was kept in ethanol for 2 hours in order to completely fill the micro and macro pores within the sample, and the final reading was recorded as ( $V_2$ ). Further, the sample soaked with ethanol was taken out of the tube and the remaining ethanol volume was measured as ( $V_3$ ). Percent porosity of individual scaffold was calculated by the formulae,  $p = (V_1 - V_3) / (V_2 - V_3) \times 100$  [Wang, Wang and Wan (2010); Xiong, Yan and Wang et al. (2002); Guan, Fujimoto and Sacks et al. (2005); Sun, Meng and Li et al. (2015)]. Instron 4467 mechanical tester with a load cell of 30kN was used to find compressive strength

and compressive modulus properties of the samples. Before testing the samples were slightly filed in order to smoothen the contact surface for compression. The load was applied at a crosshead velocity of 1mm/min with no preloading at normal room temperature conditions [Serra, Planell and Navarro (2013); Ramay and Zhang (2004)]

### ***2.3 Scanning electron microscopy, fourier transform infrared spectroscopy and x-ray diffraction analysis.***

The manufactured HA/TCP/Collagen scaffolds were examined using scanning electron microscope to see the interaction of collagen fibrils with HA/TCP particles. Also, the samples were analyzed for its macropore distribution, strand size and distance between two strands after sintering. Samples were placed on aluminum studs using double adhesive tape and were further coated with gold-palladium using JEOL JFC 1600 Auto fine coater from Japan. Pictures were taken at different magnification using JOEL-6380A scanning electron microscope [Haberstroh, Ritter and Kuschnierzet, et al. (2010)]. Transmittance mode Fourier transform infrared spectroscopy was performed to find the components of scaffold samples and also to characterize the interactions between HA/ $\beta$ -TCP and collagen fibrils. Infrared absorbance spectra of sintered HA/ $\beta$ -TCP scaffolds coated with collagen was recorded using Nicolet is5 ranging from 4000  $\text{cm}^{-1}$  to 400  $\text{cm}^{-1}$  from Thermo Scientific (Waltham, MA, USA). As an open system of measurement was used, a spectrum of atmospheric moisture was taken out without the sample and was further subtracted from the actual sample spectra to get the final plot [Sarıkaya and Aydin (2015)]. Further, crystalline phases of HA/TCP/Collagen scaffolds were examined with X-ray diffractometer (XRD). Samples were scanned from  $10^{\circ}$ - $70^{\circ}$  ( $2\theta$ ) with X'Pert PRO, PANalytical at a scan rate of 0.017  $2\theta$  with scan step time of 10.30 Sec. The copper tube was operated at 45 kV and 40 mA and the samples were rested on aluminum supports using double adhesive tape.

### ***2.4 In vitro cytotoxicity: elution method***

#### ***2.4.1 Preparation of test item extract and test procedure***

Sodium Lauryl Sulphate (SLS) (0.2 mg/mL) in 1X DMEM; (Thermo Fisher Scientific) was used as a positive control. High-Density Polyethylene Film (RM-C) (Make: Hatano Research Institute, Food and Drug Safety Centre, Japan) was used as a negative control. Dulbecco's Modified Eagle Medium with L-Glutamine 1x DMEM, New Born Calf Serum was purchased from Invitrogen. 1% Penicillin/Streptomycin solution and PBS were obtained from Himedia, India. Balb/c 3T3 was acquired from NCCS (National Center for Cell Science, Pune, India). Extraction ratio of 3  $\text{cm}^2$  of test item per milliliter of serum supplemented 1x DMEM at 37  $^{\circ}\text{C}$  for 24 h was used. The total surface area of one test item was 3.2  $\text{cm}^2$ . Test item extract was prepared by extracting ten numbers of test items (32  $\text{cm}^2$ ) in 11.7 ml (each 1 $\text{cm}^2$  of test item absorbs approximately 0.031 mL of extraction medium. Therefore, volume of 0.031 mL of extraction medium was added per each 1  $\text{cm}^2$  of test item extracted) of serum supplemented 1x DMEM for 24 h at 37  $^{\circ}\text{C}$  in an incubator. Also, negative control (High-Density Polyethylene film) measuring 6  $\text{cm}^2$  (surface area of one side is 3  $\text{cm}^2$ , both the sides were involved in extraction) was extracted in 2 mL of serum supplemented 1x DMEM at the ratio of 3  $\text{cm}^2$  per mL at 37

°C for 24 hours. At the end of extraction period, there was no change in color of the extract (pre-and post-extraction) and there were no particulates present. No additional processing such as filtration, centrifugation, pH adjustments or any other processing were made. The extract was used within 25 min and it was considered stable during this time. A series of eight different concentrations (30%, 40%, 50%, 60%, 70%, 80%, 90% and 100%) of the test item extract were prepared for the study.

Exponentially growing Balb/c 3T3 cells were trypsinized using trypsin-EDTA (Make: Sigma) and counted in a hemocytometer using 0.4% Trypan blue (Himedia, India). Exactly  $1 \times 10^5$  cells per mL was prepared (0.179 mL of cell suspension [ $39.00 \times 10^5$  cells per mL] was added to 6.821 mL of culture media to get 7 mL of cell suspension) and 100  $\mu$ L was seeded in wells B2 to G11 of 96 well plates at a concentration of  $1 \times 10^4$  cells per well. The plate was incubated in an incubator with 5% CO<sub>2</sub> at 37 °C for 24 hours. The following day, the confluence and morphology of the cell were checked and found to be greater than 70 % confluent and normal. Then the medium was removed and six replicates of appropriate concentrations of the test item extract, positive and negative controls were added to the cultures. The plate was then incubated in the CO<sub>2</sub> incubator for 24h. After 24 hours of incubation, the cells were examined under an inverted microscope for morphological evidence of cytotoxicity. Immediately following the visual assessment, wells were washed with 150  $\mu$ L of phosphate buffered saline (PBS) from Himedia. This was removed, and 100  $\mu$ L of the neutral red medium was added. The plates were then incubated in the CO<sub>2</sub> incubator for exactly 3 hours. Following the incubation, the neutral red medium was removed and the cells were washed with 150  $\mu$ L of PBS which was removed before adding 150  $\mu$ L of neutral red-solution (ethanol:glacial acetic acid: distilled water, 10 mL:0.2 mL:9.8 mL). Plates were shaken periodically until all neutral red was removed from the cells, forming a homogenous solution. The resulting colored solution was analyzed using a microplate reader (Mindray MR-96A) at a wavelength setting of 546 nm. Neutral Red absorbance was expressed in terms of absolute optical density (OD<sub>546</sub>; which was OD<sub>546</sub> of the culture minus the mean OD<sub>546</sub> of medium blanks). Cell viability was calculated as the percentage of culture OD<sub>546</sub> divided by negative control OD<sub>546</sub>.

## **2.5 Guinea pig maximization test**

### **2.5.1 Preparation of the test item extracts and test procedure**

Physiological saline (0.9% w/v sodium chloride solution) from (Baxter, India) and sesame oil (Sigma-Aldrich) was used as negative control.  $\alpha$ -Hexylcinnamaldehyde-Technical grade 85% was used as positive control. Since the test item cannot be administered per se to the animals, polar (physiological saline) and non-polar (sesame oil) extracts were freshly prepared by extracting at the rate of 3 cm<sup>2</sup> surface area of test item per milliliter of solvents at 37 °C for 72 h. As the surface area of each test item was 3.2 cm<sup>2</sup>. Eight test items measuring total 25.6 cm<sup>2</sup> were extracted in 9.3 mL of physiological saline (Each 1 cm<sup>2</sup> of the test item absorbed 0.029 ml of physiological saline hence, additional volume of 0.74 mL physiological saline was added) and another eight test items measuring total 25.6 cm<sup>2</sup> were extracted in 8.5 mL of sesame oil under sterile conditions (No absorption was recorded with sesame oil). Solvent controls were also

subjected to the same temperature and time period conditions. At the end of extraction period, there was no change in color of the extract and solvent control (pre-and post-extraction) and there were no particulates. No additional processing such as filtration, centrifugation, pH adjustments or any other processing were made. The extracts and solvent controls were transferred to sterile containers and stored at room temperature. All extracts and solvent controls were used within 6 h of preparation and were considered to be stable during this time.

Animals were divided into four groups; G-five guinea pigs for the polar solvent control, G2-ten guinea pigs for the polar test item extract, G3-five guinea pigs for the non-polar solvent control and G4-en guinea pigs for the non-polar test item extract. The fur over the treatment sites was clipped and shaved on the day of treatment, prior to dosing on all the animals. Induction of sensitization was a two-stage procedure with intradermal injections initially administered, followed by a topical patch exposure on day 7.

A pair of 0.1 mL of intradermal injections was injected into each animal, at the injection sites (A, B and C) as shown in Table.3. Intradermal injections of the test item extracts, vehicles and Freund's Complete Adjuvant (FCA) in various mixtures were administered to the negative control and test groups Table 3. On day 6, following the intradermal injections, test area was treated with 0.5 mL of 10% sodium lauryl sulfate (Thermo Fisher Scientific) along with Vaseline.n day 7, a topical patch of size 8 cm<sup>2</sup> (Modern Health Care) loaded with 0.5 mL of test item extract and negative control respectively was applied topically to respective groups of guinea pigs, on the same site as that of intradermal injections. Over the topical patch, the loose dressing was done with occlusive dressing which was held in place for 48h.

On day 21, the challenge exposure was administered as a topical patch of size 8 cm<sup>2</sup> (Modern Health Care). Patch soaked with 0.5 mL of test item extract was applied on the left side and the patch with 0.5 mL of the negative control was applied on the right side of each animal in respective groups for 24h at sites other than those used for intradermal injections/topical applications and the application sites were marked with a non-irritant permanent marker ink. The details of the experiment are summarized in Table.1.

**Table 1:** Mechanical results obtained for composite scaffolds sintered at 1250<sup>0</sup>C.

Strand Orientation	Strand Size (μm)	Dist. b/w Strands (μm)	Total Porosity( <i>p</i> ) (%)	Compressive Modulus (Mpa)	Compressive Strength (Mpa)
0° – 90°	400	1000	61.03	197.4383	9.403
0° – 45° – 90° – 135°	400	1000	64.17	226.456	11.785
0° – 108° – 216°	400	1000	76.46	160.398	7.639
0° – 60° – 120°	400	1000	60.24	204.199	9.725

**Table 2:** Results of viability and cytotoxicity.

	Negative Control	Viability in test item extract concentrations								Positive Control
		30%	40%	50%	60%	70%	80%	90%	100%	
Mean OD	0.576	0.572	0.571	0.570	0.575	0.574	0.572	0.574	0.575	0.003
SD ( $\pm$ )	0.048	0.044	0.033	0.027	0.021	0.021	0.018	0.039	0.029	0.007
CV (%)	8.3	7.7	5.8	4.7	3.7	3.7	3.1	6.8	5.0	233.3
Viability (%)	--	99.31	99.13	98.96	99.83	99.65	99.31	99.65	99.83	0.52
Cytotoxicity (%)	--	0.69	0.87	1.04	0.17	0.35	0.69	0.35	0.17	99.48

**Table3:** Test Procedure.

Group No.	Animal No. x	Sex	Treatment Group	Intradermal Induction Phase (0.1 mL)			Topical induction phase (0.5 mL using a patch) *		Challenge phase # (0.5 mL using a patch) *
				Injection I	Injection II	Injection III	10 % SLS	Treatment	
G1	1-5	M	Polar solvent control	1:1 mixture (v/v) FCA + (physiological saline)	Polar solvent alone	50% w/v formulation of the vehicle in a 1:1 mixture (v/v) FCA + (physiological saline)	Yes	Polar solvent	Polar solvent & Polar extract of Test item
G2	6-15	M	Test item in polar solvent	1:1 mixture (v/v) FCA + (physiological saline)	Test item in polar solvent	Polar extract of Test item in a 1:1 mixture (v/v) FCA + (physiological saline)	Yes	Polar extract of Test item	Polar solvent & Polar extract of Test item

G3	16-20	M	Non-polar solvent control	1:1 mixture (v/v) FCA + (Sesame oil)	Non-polar solvent alone	50% w/v formulation of the vehicle in a 1:1 mixture (v/v) FCA + (Sesame oil)	Yes	Non-polar solvent	Non-polar solvent & Non-polar extract of Test item
G4	21-30	M	Test item in non-polar solvent	1:1 mixture (v/v) FCA + (Sesame oil)	Test item in non-polar solvent	Non-polar extract of Test item in a 1:1 mixture (v/v) FCA + (Sesame oil)	Yes	Non-polar extract of Test item	Non-polar solvent & Non-polar extract of Test item

M- Male; FCA- Freund's Complete Adjuvant; SLS- Sodium Lauryl Sulphate; \* Patch area = 8 cm<sup>2</sup>; # Gauze (8 cm<sup>2</sup>) soaked in the respective preparation; Intradermal Injection was given on Day 0 at sites A, B and C; Topical application was applied on Day 7; Challenge dose was applied on Day 21; Sites A, B and C are shown below.

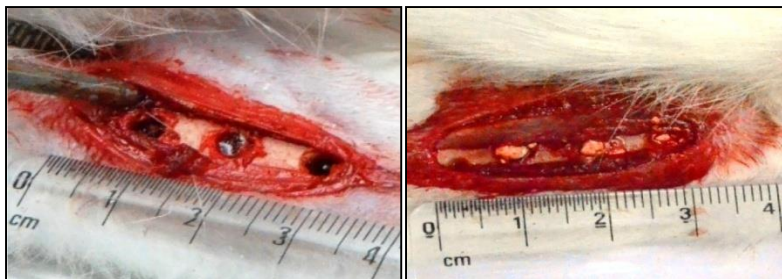
## 2.6 Animal studies

### 2.6.1 Test performance, test procedure and observations

Animals were housed under standard laboratory conditions, air-conditioned with an adequate fresh air supply (Air changes 12-15 per hour), room temperature of 20 ± 3°C, relative humidity of 30-70 %, with 12 h light and 12 h dark cycle was maintained. For housing, animals were placed in individual cages with stainless steel mesh top grill having facilities for holding pellet feed and drinking water. Reverse osmosis purified drinking water and standard laboratory feed was provided (ad libitum). Animals were acclimatized for a period of 17 days to laboratory conditions and were observed twice daily for general observations and mortality.

One day prior to the day of surgery, the animals were neatly trimmed off the fur at the tibia region of both the legs. On the day of surgery, the animals were anesthetized with Ketamine and Xylazine mixture (35mg/kg and mg/kg, respectively) through intramuscular route. The tibia region of both the legs was wiped with ethanol. Once the animals were anesthetized, a longitudinal incision was made at the tibia region and the muscle was exposed to locate the tibia bone. Three holes were bored with a driller (3mm diameter) to the tibia bone with sufficient spacing so as to accommodate three implants. HA/TCP/Collagen implants with optimum compressive strength and porosity value was machined to get cylindrical samples of size (3mm diameter, 6mm long) and were implanted into the tibia bone of the left leg of the animal and the right leg served as

sham-operated without any implant Fig.3. The whole process was performed under saline irrigation. Once the implantation procedure completed the muscle layer and the skin covering the bone tissue was sutured in layers. The area of surgery was medicated with antiseptic solution (Povidone-Iodine) and observed carefully till recovery. After the surgery, the animals were monitored for clinical signs. The total duration of the study was 77 days (17 days Acclimatization period+60 days study duration with the intermittent sacrifice of 4 animals on day 30).



(a) (b)

**Figure 3:**An example of an experimental group. (a) Control (Right Leg), (b) HA/TCP/Collagen Scaffold (Left Leg).

Individual animal body weights were recorded on initiation of acclimatization, on day 1 and weekly ( $\pm 1$  day) thereafter during the study period and on the last day before sacrificing the animals. All the animals were observed once daily for clinical signs and twice daily for mortality and morbidity. X-Ray examination of the tibia bone and the site of implantation were performed on day 30 for the G1 group animals and on day 60 for the G2 group animals. The bone was collected and preserved in 10% NBF (neutral buffered formalin) for further processing of histological evaluations. Tibia bone tissue sections were stained with H&E (Hematoxylin and Eosin) and examined under a microscope for histopathological changes. Observations for the capsule formation, inflammation, presence of polymorphonuclear cells, giant cells, plasma cells and degeneration of implant material were performed. After completion of the study, animals were sacrificed using overdosage of thiopental sodium.

### 3 Results and discussion

#### 3.1 Physical and mechanical analysis of scaffolds

Scaffolds exposed continuous interconnected compact structures with light yellow shade Fig.2. High-temperature sintering did not induce any deformations like breakage of the strands, variation in the architecture and geometry of the pores other than volumetric shrinkage. Scaffolds which measured 10mm x 10mm x 3 mm before sintering measured 9.5mm x 9.5mm x 2.85mm after sintering. All the samples showed more or less similar shrinkage after sintering. The shrinkage is caused because of first: evaporation of binder and second: diffusion of HA/TCP particles. Compression test results revealed the compressive strength of 7.639MPa for the scaffold with 0°-108°-216° lay down pattern

and 11.785 Mpa for the scaffold with 0°-45°-90°-135° lay down pattern. Scaffold with 0°-90° and 0°-60°-120° architecture showed similar strength and porosity values of 9 Mpa and 60% respectively. Although macroporosity of the scaffold with 0°-45°-90°-135° architecture is low in comparison to remaining sample architectures, increased porosity of 64.17% may be attributed to the higher percentage of microporosity associated with it which is also evident from the increasing amount of ethanol absorption by the scaffold strands. Scaffold with 0°-108°-216° architecture though has a high amount of overall porosity of 76.46% suffers from low strength property. On the basis of strength and porosity values scaffold with 0°-45°-90°-135° architecture is selected for further in-vitro and in-vivo studies Table 1. Mechanical testing of samples revealed satisfactory results for all architecture types and are comparable to the lower bounds of human cancellous bone (12MPa) Table 1. The increase in strength values can be related to the association of nanoscale (<200 µm) HA powder with TCP. However, out of the four different architectures types scaffold with 0°-45°-90°-135° lay down pattern showed relatively higher mechanical strength and optimum porosity value. HA nanopowder is used as it is established from the previous work that compared to micron scale materials nanoscale materials shows better mechanical, electrical and cytocompatible properties [Siegel and Fougere(1995)]. Furthermore, the bone which is 70% inorganic consists of hydroxyapatite crystals 20 to 80nm long and 2 to 5 nm thick [Kaplan, Hayes and Keaveny et al. (1994)]. Other elements present in the bone matrix like collagen and proteins are also in nanoscale size [Webster (2001)]. In different studies, it has been shown that nanostructured HA, ZnO, Al<sub>2</sub>O<sub>3</sub> and TiO<sub>2</sub> accelerates the calcium phosphate mineral deposition and osteoblast adhesion [Webster, Siegel and Bizios (1999); Webster, Siegel and Bizios (2000); Webster, Ergun and Doremus et al. (2000); Webster, Siegel and Bizios (2001); Webster, Ergun and Doremus et al. (2001); Gutwein and Webster (2004); Webster, Hellenmeyer and Price (2005)]. More amounts of surface microporosity, wettability and enhanced surface roughness of nanosize ceramics results in fast osseointegration of BCP ceramic with juxtapose bone. Webster et al, confirmed more amount of osteoblast and fibroblast cell adhesion on nanophase HA (67 nm) with that of micron size HA when subjected to four hours of cell culture studies [Webster, Siegel and Bizios (2000)]. In some of the in-vivo studies, it has also been highlighted that use of nanocrystalline HA coating on tantalum scaffolds significantly increased new bone growth in rat calvaria than on traditional HA-coated and uncoated scaffolds after 6 weeks of implantation [Sato (2006)].

### **3.2 FTIR, XRD and SEM analysis**

The sharp peak at 3572.75 cm<sup>-1</sup> indicated the occurrence of stretching vibrations of OH<sup>-</sup> ions in Hydroxyapatite. Also, absorption bands were around 1000, 600 and 560, which are assigned for PO<sub>4</sub><sup>3-</sup> in HA and TCP. For collagen (COO<sup>-</sup>) bands were clearly visible at 1633.41 and 1537.94 cm<sup>-1</sup> Fig. 4. XRD profile for sintered HA/TCP samples coated with collagen revealed matching peaks from 20° to 40° with that of raw powder [Sapkal, Kuthe and Kashyap et al. (2016)]. XRD pattern for HA/TCP/Collagen scaffold is shown in Fig.5. From the XRD profile it was observed that Peaks for collagen type-I did not appear because of its amorphous nature. However small peaks between 25° to 35° revealed the presence of its amorphous structure [Sarikaya and Aydin (2015)]. Also, no other phase

like calcium carbonate or calcium oxide was formed in HA/TCP sample after sintering. 3D-Bioplotting scaffolds presented a high level of interconnected pore network for all architecture types. Fig.6 shows the SEM micrograph of HA/TCP/Collagen scaffold for all architecture types. Scaffold with  $0^{\circ}$ - $90^{\circ}$  lay down pattern contained smaller channel size with larger square pores of size  $500\mu\text{m}$  when viewed from the z-axis whereas scaffold with  $0^{\circ}$ - $60^{\circ}$ - $120^{\circ}$  pattern showed smaller triangular pore of size  $413\mu\text{m}$  with bigger channels. Scaffold with the Benzene structure having  $0^{\circ}$ - $108^{\circ}$ - $216^{\circ}$  pattern showed varying pore sizes along with hexagonal pores of size  $550\mu\text{m}$ . Also, the scaffold with a staggered architecture having  $0^{\circ}$ - $45^{\circ}$ - $90^{\circ}$ - $135^{\circ}$  pattern demonstrated triangular pores of sizes  $200\mu\text{m}$  and  $420\mu\text{m}$  which appears concentric to each other. The strand diameter of all samples varied from  $344.8\mu\text{m}$  to  $380.9\mu\text{m}$  with rough surfaces having micropores from 1 to  $10\mu\text{m}$  which are supportive for the initial cell adhesion. Fig.7 displays SEM micrograph of collagen treated scaffold. Fine collagen fibrils covered HA/TCP particles partly, below which fine granulated and microporous structure is visible.

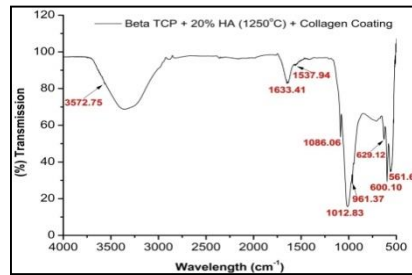


**Figure 4:** FTIR profile for HA/TCP/Collagen scaffold sintered at  $1250^{\circ}\text{C}$

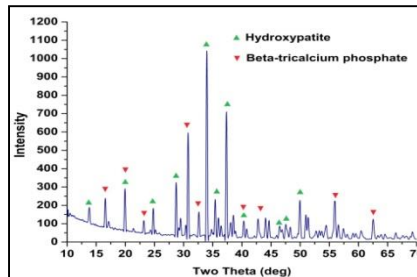


**Figure 5:** XRD pattern for HA/TCP/Collagen scaffold sintered at  $1250^{\circ}\text{C}$

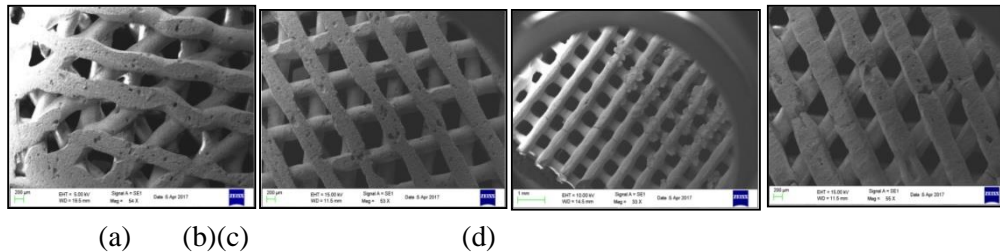


**Figure 6:** SEM micrograph of HA/TCP/Collagen scaffolds with different lay down pattern (a)  $0^{\circ}$ - $45^{\circ}$ - $90^{\circ}$ - $135^{\circ}$  (b)  $0^{\circ}$ - $108^{\circ}$ - $216^{\circ}$  (c)  $0^{\circ}$ - $90^{\circ}$  (d)  $0^{\circ}$ - $60^{\circ}$ - $120^{\circ}$  (e) Fine collagen fibrils covering HA/TCP partially.

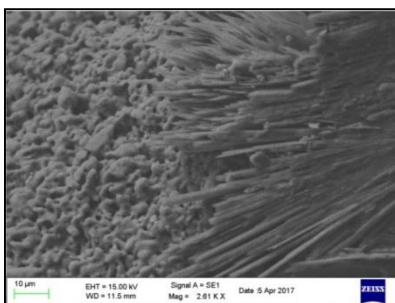


**Figure 7:** Fine collagen fibrils covering HA/TCP partially.

### 3.3 Cell cytotoxicity and skin sensitization

Before treatment, all wells had cells confluency greater than 70%. The mean  $OD_{546}$  of negative (culture media) treated cells were 0.576. The coefficient of variation for all test item extract replicate measurements were  $< 15\%$ . A clear increase in cytotoxicity was observed in the positive control treated cultures. But, no such cell destruction was evident in the negative control. Hence the assay was considered valid. It is clear that the test item extract was not-cytotoxic. Neutral red uptake assay reflects the results of qualitative analysis Table 2. HA/TCP/Collagen scaffolds for bone tissue engineering extract at concentrations 30%, 40%, 50%, 60%, 70%, 80%, 90%, and 100% showed viability greater than 70%.

Positive control trial which is conducted within the test facility after every three months gave a positive result of grade 2 moderate and confluent erythema. No response was observed in negative control treated animals. Therefore, the assay was considered valid. All the animals showed an increase in body weight at the end of the experiment. No mortality and morbidity were observed in any of the animals used in this study. The results of grading of skin reactions performed at 24 h and 48 h after removing the challenging patch are given in Table 4. Erythema at site 1 and site 3 of the intradermal injection was observed in all the animals. No sensitization reactions were observed in animals treated with the negative control. No evidence of sensitization was seen in any of the test items extracts treated animals, as no skin reactions were observed. The grading was done with Magnusson and Kligman scale.

**Table 4:** Results of grading of skin reaction after removal of the challenge patch

Group	Sex	Animal No.	Magnusson and Kligman Scale			
			24 h		48 h	
			C	T	C	T
G1	M	1	0	0	0	0
		2	0	0	0	0
		3	0	0	0	0
		4	0	0	0	0
		5	0	0	0	0
G2	M	6	0	0	0	0
		7	0	0	0	0

		8	0	0	0	0
		9	0	0	0	0
		10	0	0	0	0
		11	0	0	0	0
		12	0	0	0	0
		13	0	0	0	0
		14	0	0	0	0
		15	0	0	0	0
		16	0	0	0	0
G3	M	17	0	0	0	0
		18	0	0	0	0
		19	0	0	0	0
		20	0	0	0	0
		21	0	0	0	0
		22	0	0	0	0
		23	0	0	0	0
		24	0	0	0	0
G4	M	25	0	0	0	0
		26	0	0	0	0
		27	0	0	0	0
		28	0	0	0	0
		29	0	0	0	0
		30	0	0	0	0

M-Male; C-Control site; T-Treated site; h-hour.

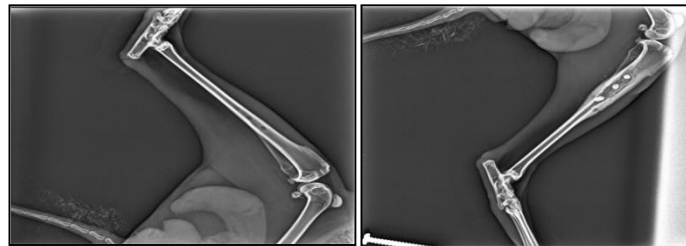
### 3.4 Animal studies

#### 3.4.1 Body weight, clinical signs observations, physiological examinations and histopathology

No change in body weight and body weight gain was observed during the study period. However, an increase in body weight was observed throughout the study period. The summary of animal body weights is presented in Table 5. Further, no abnormal clinical signs were observed during the study period. All the animals were observed to be normal. No abnormalities were observed at the site of implantation. After X-ray examination of bone on day 30 and day 60, the white colored holes showing the implant in left tibia bone while black colored empty holes were showing sham-operated right tibia bone. There was no deformity of bone observed in all the animals. X- Ray examination of the tibia bone for animal 1 is presented in the Fig.8 & Fig.9. It was evident from the histopathology results that there was a significant change in  $\beta$ -TCP + 20% hydroxyapatite treatment group compared to the control (Blank) group. The treatment group showed significant lesions characterized by the progressive new bone formation in the trephined areas, from 30th to 60th day showing well-formed bony trabeculae & good osteoblastic activity Fig. 10, 11, 12 & 13.



(a) Animal 1: Right Leg (b) Animal 1: Left Leg  
**Figure 8:** Individual animal x-ray photographs (day 30).



(a) Animal 4: Right Leg (b) Animal 4: Left Leg  
**Figure 9:** Individual animal x-ray photographs (day 60).

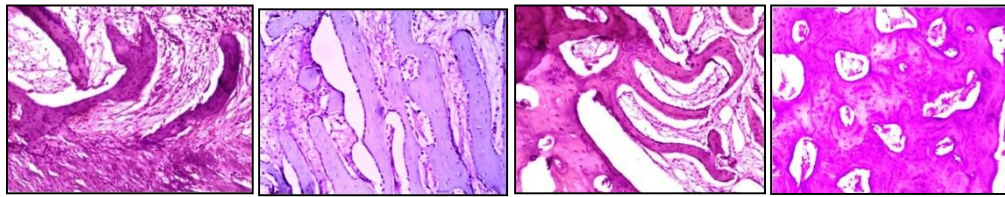
**Table 5:** Summary of body weights (kg).

Groups	Days										
	01	08	15	22	29	30	36	43	50	57	61
G1	2.60	2.70	2.73	2.78	2.90	2.93	-	-	-	-	-
	±0.08	±0.08	±0.13	±0.17	±0.22	±0.19	-	-	-	-	-
G2	2.53	2.58	2.68	2.70	2.75	2.70	2.78	2.83	2.93	2.95	2.70
	±0.05	±0.10	±0.17	±0.14	±0.21	±0.22	±0.17	±0.22	±0.22	±0.21	±0.22

Values are expressed as Mean ± standard deviation.

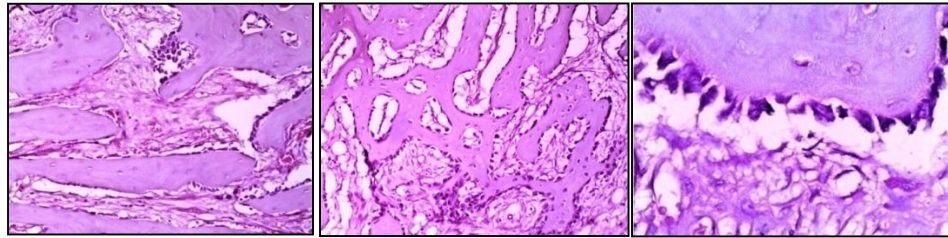
For all animals, the trephined areas in right leg (Blank) were filled with newly formed bony trabeculae lined by flattened to prominent osteoblast's Fig.10 & 12. However, the right leg of animal 1, 2 and 3 showed very well formed periosteal layer in the lesional tissue. Also, the thickness of the bony trabeculae was moderate in size & in between the bony trabeculae loose connective tissues were observed. Occasionally, multifocal osteoclasts were observed. There were no signs of mineralization throughout the lesion. Newly formed trabeculae also showed osteocytes located within the lacunae. Furthermore, in animal 4,5,6,7 and 8 (Right Leg) a moderate amount of granulation tissue was observed, though it did not reveal the lesion in the section. The lesional tissue of left leg (Treatment group) in animal 1, 2 and 3 showed moderately thick periosteal layer and the trephined areas were filled with large plate / new bony trabeculae lined by a round shaped osteoblasts. The amount of granulation tissue was moderate in formation and was seen between the trabeculae in a loose fashion. Hydroxyapatite materials were also seen at the

site of the lesion Fig.11. In animal 2 and 3 (Left Leg) no inflammatory cell infiltration and no osteoclastic activity were observed, though occasionally, plasma cells were observed. For animal 4,5,6,7 and 8 (Left Leg), an appreciable improvement in new bone formation characterized by conjoint or broad bony tissues lined with flattened osteoblasts & well-formed vascular system was observed Fig.11 &13. Occasional areas showed newly forming bony trabeculae with persistent osteoblastic activity. There were no signs of inflammation in the lesional tissue. Hydroxyapatite materials were found in the lesional areas of animal 4, 5 and 6 (Left Leg). Broader bony plates were observed in animal 7 & 8 (Left Leg) but hydroxyapatite material and osteoclastic activities were not observed.

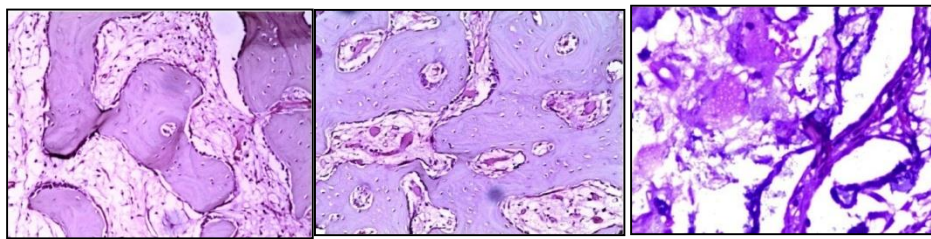


Animal 1: Moderately thick bony Trabeculae with loose connective tissue (Right Leg)  
 Animal 2: Moderately sized Bony Trabeculae (Right Leg)  
 Animal 3: Incomplete Trabeculae formation (Right Leg)  
 Animal 6: Well formed bony trabeculae(Right Leg).

**Figure 10:** Histology sections of control specimens after 30 days.



Animal 1: Thick bony Trabeculae with loose connective tissue (Left Leg).  
 Animal 2: New Bony Trabeculae lined by round shaped Osteoblasts (Left Leg).  
 Animal 3: Newly formed bony Trabeculae lined by flattened to prominent Osteoblast (Left Leg).



Animal 6: Conjoint or broad bony tissue lined with flattened Osteoblasts (Left Leg).  
 Animal 6: Well developed Vascular System (Left Leg).  
 Animal 2: Hydroxyapatite material in the lesion (Left Leg).

**Figure 11:** Histology sections of Ha/TCP/Collagen specimens after 30 days.

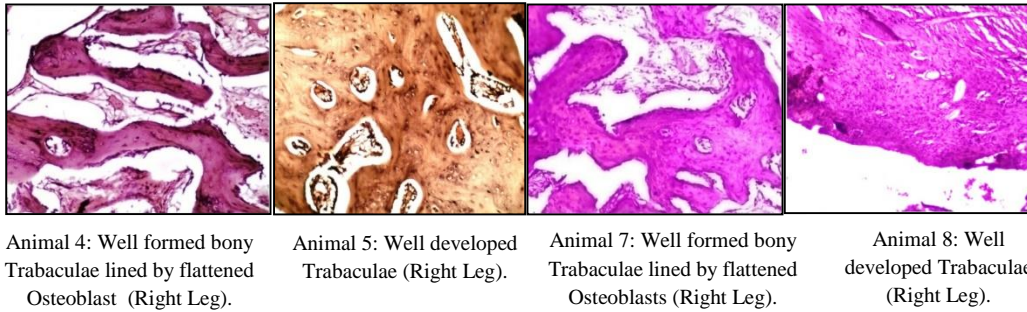


**Figure 12:** Histology sections of control specimens after 60 days.

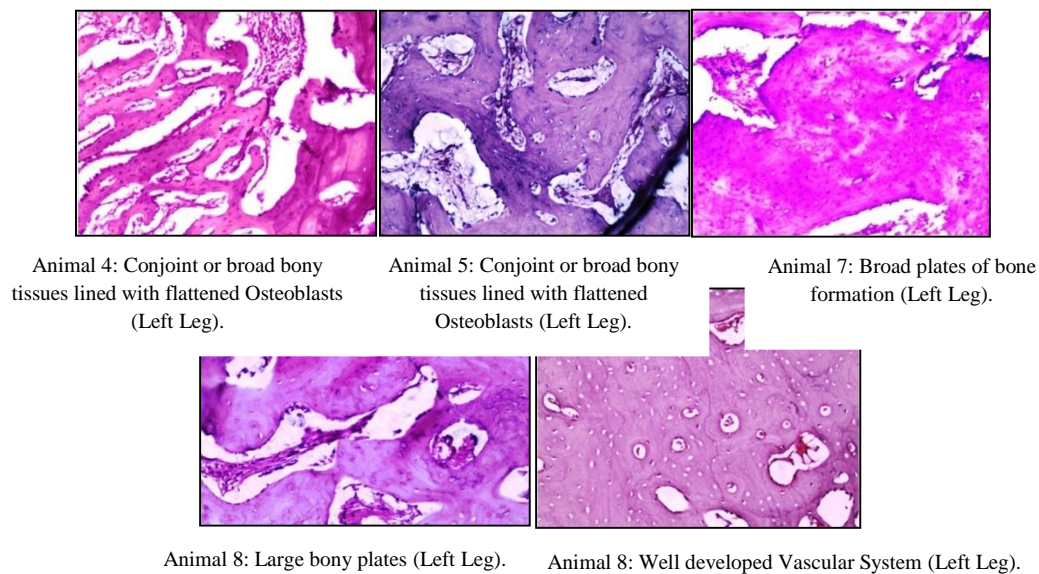


**Figure 13:** Histology sections of Ha/TCP/Collagen specimens after 60 days.

#### 4 Conclusion

In the present study, a through bone defect was created in Rabbit Tibia bone in order to evaluate HA/TCP/Collagen as a bone graft substitute and discovered the role of scaffold architecture on mechanical stability and overall porosity in order to suit it for the load bearing applications. Based on the results of the present study, the test item  $\beta$ -TCP + 20% Hydroxyapatite/Collagen scaffold with 0°-45°-90°-135° lay down pattern showed the utmost mechanical strength value with optimum porosity level. Cytotoxicity results showed more than 70% viability in all sample types towards Balb/c 3T3 cell line. The extracts prepared from the test items did not show any sensitivity to Guinea pig skin. Further, the implants showed high biocompatibility with rabbit tibia bone. Increase in body weight was observed in all animals throughout the experiment. There was observed no abnormality or deformity in the tibia bone when examined under X-rays after 30 and 60 days. The treatment group showed significant lesions characterized by the progressive

new bone formation in the trephined areas, from 30th to 60th day showing well-formed bony trabeculae & good osteoblastic activity.

## 5 Conflict of interest and financial disclosure

The authors declare that they have no conflict of interest. The research is jointly funded by the State Government of Maharashtra (Rajiv Gandhi S&T Commission) and Central Government of India (Department of S&T), New Delhi.

## References

- Albee, F. H.**(1920): Studies in bone growth: Triple calcium phosphate as a stimulus to osteogenesis, *Ann Surg*, vol. 71, no. 1, pp.32-36.
- Aoki, H.** (1994): *Medical Applications of Hydroxyapatite*, IshiyakuEuroamerica, Inc: Tokyo.
- Chen,Z.;Li, D.;Lu, B.; Tang, Y.;Sun, M.; Xu, S.**(2005): Fabrication of osteo-structure analogous scaffolds via fused deposition modeling, *Scr. Mater*, vol.52, no.2, pp.157-161.
- Crigel, M.H., Balligand, M.** (2002): Critical size defect model on the femur in rabbits, *Vet Comp OrthopTraumatol*, vol. 15, no. 3, pp.158-163.
- Daculsi,G.; LeGeros, R.Z.; Nery, E.; Lynch, K.;Kerebel, B.**(1989): Transformation of biphasic calcium phosphate ceramics*in vivo*: ultrastructural and physicochemical characterization”, *J Biomed Mat Res*, vol. 23, pp. 883-894.
- Daculsi, G.; LeGerosRZ;Grimandi, G.; Soueidan, A.;LeGeros, J.** (2008): Effect of Sintering Process of HA/TCP (BCP) Bioceramics on Microstructure, Dissolution and Cell Proliferation, *Key Engineering Materials*, vol. 361-363, pp.1139-1142.
- Daculsi, G. and Dard, M.** (1994): Bone-Calcium-Phosphate ceramic interface, *Osteosynthese International 2*, pp.153-156.
- DeGroot, K.** (1983): Ceramics of calcium phosphates: Preparation and properties. In: DeGroot K (Ed). *Bioceramics of Calcium Phosphate*. CRC Press: Boca Raton, pp.100-114.
- Goyenvalle, E.;Aguado, E.;Legeros, R.;Daculsi, G.** (2007): Effect of Sintering Process on Microporosity, and bone growth on Biphasic Calcium Phosphate Ceramics, *Key Engineering Materials*, vol. 333-334.
- Guan, J.; Fujimoto, K.; Sacks, M. and Wagner, W.** (2005): Preparation and characterization of highly porous, biodegradable polyurethane scaffolds for soft tissue applications, *Biomaterials*, vol.26, no.18, pp.3961-3971.
- Gutwein, L. G. and Webster, T. J.** (2004): Increased viable osteoblast density in the presence of nanophase compared to conventional alumina and titania particles, *Biomaterials*, vol. 25, pp.4175-4183.
- Haberstroh K.; Ritter K.; Kuschnierz J.; Bormann KH.;Kaps C.; Carvalho C.; Mülhaupt R.; Sittinger M. andGellrich NC.** (2010): Bone repair by cell-seeded 3D-bioplotting composite scaffolds made of collagen treated tricalciumphosphate or

tricalciumphosphate-chitosan-collagen hydrogel or PLGA in ovine critical-sized calvarial defects, *J Biomed Mater Res B Appl Biomater*, vol. 93, no. 2, pp.520-530.

**Hench, L. L. and Wilson, J.**(1993):An Introduction to Bioceramics, *World Scientific*, vol. 1.

**Hench, L. L.**(1998): Bioceramics, *Journal of the American Ceramic Society*, vol.81, no.7, pp.1705-1728.

**Hollinger, J.O. and Kleinschmidt, J.C.** (1990): The critical size defect as an experimental model to test bone repair materials”, *J.CraniofacSurg*, vol.1, no.1, pp.60-68.

**Joon B. Park and Joseph D. Bronzino.** (2003): Biomaterials: Principles and Applications, *CRC Press*, New York.

**Jarcho, M.** (1981): Calcium phosphate ceramics as hard tissue prosthetics, *ClinOrthopaed*, vol.157, pp.259-278.

**Kaplan, F. S.; Hayes, W. C.; Keaveny, T. M.; Boskey, A.; Einhorn, T. A. and Iannotti, J. P.** (1994): Form and function of bone. *Orthopedic basic science*, pp.127-185, S. P. Sinmon, (eds.), American Academy of Orthopaedic Surgeons.

**LeGeros, R.Z.** (2002): Properties of osteoconductive biomaterials: calcium phosphates, *ClinOrthopaedRel Res*, vol.395, pp.81-98.

**Livingston Arinzeh, T.; Peter, S.; Archambault, M.; Van Den Bos, C.; Gordon, S.; Kraus, K.; Smith, A., Kadiyala, S.**(2003): Allogeneic mesenchymal stem cells regenerate bone in a critical- sized canine segmental defect, *Journal of Bone and Joint Surgery American*, vol.85-A, no.10, pp.1927-1935.

**Livingston, T.L.; Gordon, S.; Archambault, M.; Kadiyala, S.; McIntosh, K.; Smith, A., Peter, S.J.** (2003): Mesenchymal stem cells combined with biphasic calcium phosphate ceramics promote bone regeneration, *J Mater Sci Mater Med*, vol.14, no.3, pp. 211-218.

**Piconi, C.; Maccauro.**(1999): Zirconia as a ceramic biomaterial, *Biomaterials*, vol.20, no.1, pp.1-25.

**Ratner, B. D.; Hoffman, A. S.; Schoen, F. J and Lemons, J. E**(2004): Biomaterials Science-An Introduction to Materials in Medicine, 2nd edition, *Academic Press*, New York, pp.526.

**de Oliveira, R.; Lomelino, L.L.; Castro-Silva, A.B.; Linhares, G.G.; Alves, S.R. et al.**(2012): The association of human primary bone cells with biphasic calcium phosphate ( $\beta$ TCP/HA 70: 30) granules increases bone repair, *J. Mater. Sci. Mater. Med*, vol.23, no.3, pp.781-788.

**Ramay, H. R. R.; Zhang, M.**(2004): Biphasic calcium phosphate nanocomposite porous scaffolds for load-bearing bone tissue engineering, *Biomaterials*, vol.25, no.21, pp. 5171-5180.

**Sapkal, P.; Kuthe, A.; Kashyap, R.; Nayak, A.; Kuthe, S. and Kawle, A.** (2016): Indirect fabrication of hydroxyapatite/b-tricalcium phosphate scaffold for osseous tissue formation using additive manufacturing technology, *Journal of Porous Materials*, vol.23, no.6, pp.1567-1574.

- Sapkal, P.; Kuthe, A.; Kashyap, R.; Nayak, A.;Kuthe, S. and Kawle, A.** (2016): Indirect casting of patient-specific tricalcium phosphate zirconia scaffolds for bone tissue regeneration using rapid prototyping methodology, *Journal of Porous Materials*, pp.1-11.
- Sato, M.**(2006): Nanophase hydroxyapatite coatings for dental and orthopedic applications [Ph.D. thesis]. School of Materials Engineering, Purdue University, West Lafayette, IN, USA.
- Sarkar. S. K.andLee. B. T.** (2015): Hard tissue regeneration using bone substitutes: an update on innovations in materials, *Korean J. Intern. Med*, vol.30, no.3, pp.279-293.
- Sarikaya, B.; Aydin, H. M.** (2015): Collagen/Beta-Tricalcium Phosphate Based Synthetic Bone Grafts via Dehydrothermal Processing, *BioMed Research International*, vol.2015.
- Serra. T;Planell. J. A.; Navarro. M.**(2013): High-resolution PLA-based composite scaffolds via 3-D printing technology, *Acta Biomater*, vol. 9, no.3, pp.5521-5530.
- Sharaf, B.; Faris, C.B.; Abukawa, H.; Susarla. S. M.; Vacanti. J. P; Kaban, L. B.; Troulis, M.J.** (2011): Three-dimensionally printed polycaprolactone and  $\beta$ -tricalcium phosphate scaffolds for bone tissue engineering: an in vitro study, *Oral Maxillofac. Surg*, vol.70, no.3, pp.647-656.
- Siegel, R. W.; Fougere, G. E.** (1995): Mechanical properties of nanophase metals, *Nanostruct. Mater*, vol.6, pp.205-216.
- Sun, A.; Meng, Q.; Li, W.; Liu. S. and Chen. W.**(2015): Construction of tissue-engineered laryngeal cartilage with a hollow, semi-flared shape using poly (3-hydroxybutyrate-co-3-hydroxyhexanoate), *Experimental and therapeutic medicine*, vol.9, No.4, pp.1482-1488.
- Sun. W and Lal. P.** (2002): Recent development on computer-aided tissue engineering-a review", *Comput. Methods Programs Biomed*, vol.67, pp.85-103.
- Valiathan, M. S. and Krishnan, V. K.** (1999): Biomaterial: An Overview, *Nation. Med. J. Ind*, vol.12, no. 6, pp. 270-274.
- Wang. Q; Wang. Q; Wan. C.** (2010): The effect of porosity on the structure and properties of calcium polyphosphate bioceramics, *Ceramics-Silikaty*, vol.55, no.1, pp.43-48.
- Webster, T. J.** (2001): *Nanophase Ceramics: The future orthopedic and dental implant material*", *Advances in Chemical Engineering*, J. Y. Ying (eds.), Academic Press: A Harcourt Science and Technology company, pp.125-166.
- Webster, T. J.; Siegel, R. W.; Bizios, R.** (1999): Osteoblast adhesion on nanophase ceramics, *Biomaterials*, vol.20, no.13, pp. 1221-1227.
- Webster, T. J.; Siegel, R. W.; Bizios, R.** (1999): Design and evaluation of nanophase alumina for orthopaedic/dental applications, *Nanostructured Materials*, vol.12, pp.983-986.
- Webster, T. J.; Siegel, R. W.; Bizios, R.** (2000): Specific proteins mediate osteoblast adhesion on nanophase ceramics, *J. Biomed. Mater. Res*, Vol.51, pp.475-483.
- Webster, T. J.; Ergun, C.; Doremus, R. H.; Seigel, R.W.; Bizios, R.** (2000): Enhanced

functions of osteoblasts on nanophase ceramics, *Biomaterials*, vol.21, pp.1803-1810.

**Webster, T. J.; Siegel, R. W.; Bizios, R.** (2001): Nanoceramic surface roughness enhances osteoblast and osteoclast functions for improved orthopedic/dental implant efficacy, *Scripta Mater*, vol.44, pp.1639-642.

**Webster, T. J.; Ergun, C.; Doremus, R. H.; Seigel, R. W. and Bizios, R.** (2001): Enhanced osteoclast-like functions on nanophase ceramics, *Biomaterials*, vol.22, pp.1327-1333.

**Webster, T. J.; Hellenmeyer, E. L. and Price, R. L.** (2005): Increased osteoblast functions on theta+delta nanofiber alumina, *Biomaterials*, vol.26, pp.953-960.

**Webster, T. J.; Siegel, R. W.; Bizios, R.** (2000): Specific proteins mediate osteoblast adhesion on nanophase ceramics, *J. Biomed. Mater. Res*, vol.51, pp. 475-483.

**Xiong, Z.; Yan, Y.; Wang, S.; Zhang, R.; Zhang, C.** (2002): Fabrication of porous scaffolds for bone tissue engineering via low-temperature deposition, *Scr. Mater*, vol.46, pp.771-776.

**Yang, S.; Leong K.F.; Du, A. and Chua, C.K.** (2001): The design of scaffolds for use in tissue engineering. Part I. Traditional factors, *Tissue Eng*, vol. 7, no. 6, pp. 679-689.

**Ye, X.; Yin, X.; Yang, D.; Tan, J. and Liu, G.** (2012): Ectopic bone regeneration by human bone marrow mononucleated cells, undifferentiated and osteogenically differentiated bone marrow mesenchymal stem cells in beta-tricalcium phosphate scaffolds, *Tissue Eng Part C Methods*, vol.18, no.7, pp.545-556.

**Zein, I.; Hutmacher, D. W.; Tan, K. C.; Teoh, S. H.**(2002): Fused deposition modeling of novel scaffold architectures for tissue engineering applications, *Biomaterials*, vol.23, no.4, pp.1169–1185.